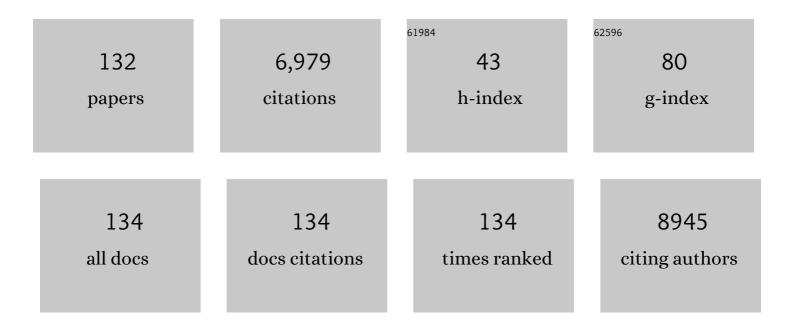
List of Publications by Year in descending order

Source: https://exaly.com/author-pdf/6647746/publications.pdf Version: 2024-02-01



#	Article	IF	CITATIONS
1	Preparation and analysis of pyroligneous liquor, charcoal and gas from lacquer wood by carbonization method based on a biorefinery process. Energy, 2022, 239, 121918.	8.8	2
2	Ultraviolet Photodetectors Based on Dimetallofullerene Lu ₂ @ <i>C_s</i> (6)-C ₈₂ Nanorods. ACS Applied Nano Materials, 2022, 5, 1683-1689.	5.0	8
3	Reversible Threeâ€Color Fluorescence Switching of an Organic Molecule in the Solid State via "Pump–Trigger―Optical Manipulation. Angewandte Chemie, 2022, 134, .	2.0	6
4	Reversible Threeâ€Color Fluorescence Switching of an Organic Molecule in the Solid State via "Pump–Trigger―Optical Manipulation. Angewandte Chemie - International Edition, 2022, 61, .	13.8	27
5	The composition, physicochemical properties, antimicrobial and antioxidant activity of wood vinegar prepared by pyrolysis of Eucommia ulmoides Oliver branches under different refining methods and storage conditions. Industrial Crops and Products, 2022, 178, 114586.	5.2	13
6	Demand-oriented construction of Mo3S13-LDH: A versatile scavenger for highly selective and efficient removal of toxic Ag(I), Hg(II), As(III), and Cr(VI) from water. Science of the Total Environment, 2022, 820, 153334.	8.0	14
7	Turn-on green fluorescence imaging for latent fingerprint applications. Materials Chemistry Frontiers, 2022, 6, 1188-1193.	5.9	13
8	Cationic Conjugated Polyelectrolytes with Aggregationâ€Induced Ratiometric Fluorescence. Macromolecular Rapid Communications, 2022, , 2100899.	3.9	1
9	Hydrogel loading 2D montmorillonite exfoliated by anti-inflammatory Lycium barbarum L. polysaccharides for advanced wound dressing. International Journal of Biological Macromolecules, 2022, 209, 50-58.	7.5	12
10	Nature-inspired nanozymes as signal markers for in-situ signal amplification strategy: A portable dual-colorimetric immunochromatographic analysis based on smartphone. Biosensors and Bioelectronics, 2022, 210, 114289.	10.1	27
11	AIE-based fluorescent micro-optical sectioning tomography for automatic 3D mapping of β-amyloid plaques in Tg mouse whole brain. Chemical Engineering Journal, 2022, 446, 136840.	12.7	9
12	Deep eutectic solvents in the extraction of active compounds from Eucommia Ulmoides Oliv. leaves. Journal of Food Measurement and Characterization, 2022, 16, 3410-3422.	3.2	7
13	Visible-light-induced scission and rapid healing of polyurethane elastomers based on photoswitchable hexaarylbiimidazole units. Materials Chemistry Frontiers, 2021, 5, 1364-1372.	5.9	6
14	Poly[N-(2-acetamidoethyl)acrylamide] supramolecular hydrogels with multiple H-bond crosslinking enable mouse brain embedding and expansion microscopy. Materials Chemistry Frontiers, 2021, 5, 1795-1805.	5.9	0
15	Vapor selenization produced Bi ₂ Se ₃ nanoparticles in carbon fiber 3D network as binder-free anode for flexible lithium-ion batteries. Materials Chemistry Frontiers, 2021, 5, 2832-2841.	5.9	21
16	Carborane photochromism: a fatigue resistant carborane switch. Chemical Communications, 2021, 57, 9466-9469.	4.1	6
17	The effects of pyrolysis temperature and storage time on the compositions and properties of the pyroligneous acids generated from cotton stalk based on a polygeneration process. Industrial Crops and Products, 2021, 161, 113226.	5.2	10
18	Hydrophilic AIE-Active Tetraarylethenes for Fluorescence Sensing and Super-Resolution Imaging of Amyloid Fibrils from Hen Egg White Lysozyme. ACS Applied Materials & Interfaces, 2021, 13, 19625-19632.	8.0	15

#	Article	IF	CITATIONS
19	Carboxymethylation of polysaccharide isolated from Alkaline Peroxide Mechanical Pulping (APMP) waste liquor and its bioactivity. International Journal of Biological Macromolecules, 2021, 181, 211-220.	7.5	17
20	Valorization of tree leaves waste using microwaveâ€assisted hydrothermal carbonization process. GCB Bioenergy, 2021, 13, 1690-1703.	5.6	5
21	Visible-light-driven isotropic hydrogels as anisotropic underwater actuators. Nano Energy, 2021, 85, 105965.	16.0	57
22	Photomechanical polymer hydrogels based on molecular photoswitches. Journal of Polymer Science, 2021, 59, 2246-2264.	3.8	22
23	Unraveling Dual Aggregationâ€Induced Emission Behavior in Stericâ€Hindrance Photochromic System for Super Resolution Imaging. Angewandte Chemie - International Edition, 2020, 59, 8560-8570.	13.8	93
24	Boosted charge transfer and Na-ion diffusion in cooling-fins-like Sb2Te3–Te nano-heterostructure for long cycle life and high rate capability anode. Nano Energy, 2020, 70, 104468.	16.0	54
25	AlE-Based Dynamic <i>in Situ</i> Nanoscale Visualization of Amyloid Fibrillation from Hen Egg White Lysozyme. Bioconjugate Chemistry, 2020, 31, 2303-2311.	3.6	13
26	Visible-Light-Driven Photoswitching of Aggregated-Induced Emission-Active Diarylethenes for Super-Resolution Imaging. ACS Applied Materials & amp; Interfaces, 2020, 12, 27651-27662.	8.0	65
27	Real-Time Fluorescence <i>In Situ</i> Visualization of Latent Fingerprints Exceeding Level 3 Details Based on Aggregation-Induced Emission. Journal of the American Chemical Society, 2020, 142, 7497-7505.	13.7	142
28	Photoplastic Self-Healing Polyurethane Springs and Actuators. Chemistry of Materials, 2019, 31, 5081-5088.	6.7	29
29	Long cycle life and high rate capability of three dimensional CoSe2 grain-attached carbon nanofibers for flexible sodium-ion batteries. Nano Energy, 2019, 58, 715-723.	16.0	182
30	Photoplastic Transformation Based on Dynamic Covalent Chemistry. ACS Applied Materials & amp; Interfaces, 2019, 11, 23623-23631.	8.0	18
31	Deciphering Erasing/Writing/Reading of Near-Infrared Fluorophore for Nonvolatile Optical Memory. ACS Applied Materials & Interfaces, 2019, 11, 23750-23756.	8.0	23
32	Comparative Evaluation of Hydrothermal Carbonization and Low Temperature Pyrolysis of Eucommia ulmoides Oliver for the Production of Solid Biofuel. Scientific Reports, 2019, 9, 5535.	3.3	47
33	Geminal Cross Coupling (GCC) Reaction for AIE Materials. Chinese Journal of Polymer Science (English) Tj ETQq1	l <u>9.7</u> 8431	4 ₅ gBT /Ove
34	AIE-based universal super-resolution imaging for inorganic and organic nanostructures. Materials Horizons, 2018, 5, 474-479.	12.2	29
35	Towards high-performance cathode materials for lithium-ion batteries: Al2O3-coated LiNi0.8Co0.15Zn0.05O2. Journal of Solid State Electrochemistry, 2018, 22, 2395-2403.	2.5	24
36	A novel high-performance self-powered UV-vis-NIR photodetector based on a CdS nanorod array/reduced graphene oxide film heterojunction and its piezo-phototronic regulation. Journal of Materials Chemistry C, 2018, 6, 630-636.	5.5	59

#	Article	IF	CITATIONS
37	Codensification of Agroforestry Residue with Bio-Oil for Improved Fuel Pellets. Energy & Fuels, 2018, 32, 598-606.	5.1	21
38	Geminal cross-coupling synthesis, ion-induced emission and lysosome imaging of cationic tetraarylethene oligoelectrolytes. Chemical Communications, 2018, 54, 3617-3620.	4.1	6
39	In2O3 nanoparticles/carbon fiber hybrid mat as free-standing anode for lithium-ion batteries with enhanced electrochemical performance. Journal of Alloys and Compounds, 2018, 735, 319-326.	5.5	34
40	Chemical constituents and antimicrobial activity of wood vinegars at different pyrolysis temperature ranges obtained from <i>Eucommia ulmoides</i> Olivers branches. RSC Advances, 2018, 8, 40941-40949.	3.6	25
41	Graphene-like MoS ₂ Nanosheets on Carbon Fabrics as High-Performance Binder-free Electrodes for Supercapacitors and Li-Ion Batteries. ACS Omega, 2018, 3, 17466-17473.	3.5	39
42	Photoswitchable Selfâ€Assembly/Disassembly of Nearâ€Infrared Fluorophores. Chemistry - A European Journal, 2018, 24, 16251-16256.	3.3	9
43	Progress on photochromic diarylethenes with aggregation induced emission. Frontiers of Optoelectronics, 2018, 11, 317-332.	3.7	20
44	Both self-assembly and aggregation-induced emission are photoswitchable. Science China Chemistry, 2018, 61, 1201-1202.	8.2	4
45	Tellurium nanotubes grown on carbon fiber cloth as cathode for flexible all-solid-state lithium-tellurium batteries. Electrochimica Acta, 2018, 282, 870-876.	5.2	38
46	AIE-based super-resolution imaging probes for β-amyloid plaques in mouse brains. Materials Chemistry Frontiers, 2018, 2, 1554-1562.	5.9	68
47	Piezo-phototronic effect modulated self-powered UV/visible/near-infrared photodetectors based on CdS:P3HT microwires. Nano Energy, 2017, 34, 155-163.	16.0	84
48	PEGylated Perylenemonoimide-Dithienylethene for Super-Resolution Imaging of Liposomes. ACS Applied Materials & Interfaces, 2017, 9, 10338-10343.	8.0	26
49	Nanosized-bismuth-embedded 1D carbon nanofibers as high-performance anodes for lithium-ion and sodium-ion batteries. Nano Research, 2017, 10, 2156-2167.	10.4	172
50	Hierarchical CuBi ₂ O ₄ microspheres as lithium-ion battery anodes with superior high-temperature electrochemical performance. RSC Advances, 2017, 7, 13250-13256.	3.6	29
51	Super-resolution imaging of self-assembly of amphiphilic photoswitchable macrocycles. Chemical Communications, 2017, 53, 2669-2672.	4.1	13
52	Self-standing Bi ₂ O ₃ nanoparticles/carbon nanofiber hybrid films as a binder-free anode for flexible sodium-ion batteries. Materials Chemistry Frontiers, 2017, 1, 1615-1621.	5.9	73
53	Ultrasensitive water sensors based on fluorenone-tetraphenylethene AIE luminogens. Materials Chemistry Frontiers, 2017, 1, 1841-1846.	5.9	46
54	Flexible high-energy asymmetric supercapacitors based on MnO@C composite nanosheet electrodes. Journal of Materials Chemistry A, 2017, 5, 804-813.	10.3	49

#	Article	IF	CITATIONS
55	Hollow porous CuO/C composite microcubes derived from metal-organic framework templates for highly reversible lithium-ion batteries. Journal of Alloys and Compounds, 2017, 706, 97-102.	5.5	70
56	Solid-State Photoinduced Luminescence Switch for Advanced Anticounterfeiting and Super-Resolution Imaging Applications. Journal of the American Chemical Society, 2017, 139, 16036-16039.	13.7	323
57	Photoswitchable polyfluorophores based on perylenemonoimide–dithienylethene conjugates as super-resolution MitoTrackers. Journal of Materials Chemistry C, 2017, 5, 9339-9344.	5.5	11
58	Bulky 4,6-disubstituted tetraphenylethene–naphthalimide dyad: synthesis, copolymerization, stimuli-responsive fluorescence and cellular imaging. Faraday Discussions, 2017, 196, 439-454.	3.2	14
59	Highâ€Performance Fiberâ€Shaped Allâ€Solidâ€State Asymmetric Supercapacitors Based on Ultrathin MnO ₂ Nanosheet/Carbon Fiber Cathodes for Wearable Electronics. Advanced Energy Materials, 2016, 6, 1501458.	19.5	409
60	Monodisperse AlEâ€Active Conjugated Polymer Nanoparticles via Dispersion Polymerization Using Geminal Crossâ€Coupling of 1,1â€Dibromoolefins. Small, 2016, 12, 6547-6552.	10.0	26
61	Single-wavelength-controlled in situ dynamic super-resolution fluorescence imaging for block copolymer nanostructures via blue-light-switchable FRAP. Photochemical and Photobiological Sciences, 2016, 15, 1433-1441.	2.9	20
62	Isolation and analysis of four constituents from barks and leaves of Eucommia ulmoides Oliver by a multi-step process. Industrial Crops and Products, 2016, 83, 124-132.	5.2	41
63	Twofold photoswitching of NIR fluorescence and EPR based on the PMI–N–HABI for optical nanoimaging of electrospun polymer nanowires. Journal of Materials Chemistry C, 2016, 4, 2498-2505.	5.5	17
64	The synthesis and aggregation-induced near-infrared emission of terrylenediimide–tetraphenylethene dyads. Chemical Communications, 2016, 52, 5808-5811.	4.1	30
65	Synthesis of Fluoreneâ€Bridged Arylene Vinylene Fluorophores: Effects of Endâ€Capping Groups on the Optical Properties, Aggregation Induced Emission. Chinese Journal of Chemistry, 2015, 33, 939-947.	4.9	10
66	Optical Nanoimaging for Block Copolymer Self-Assembly. Journal of the American Chemical Society, 2015, 137, 2436-2439.	13.7	83
67	Antiphase Dual-Color Correlation in a Reactant–Product Pair Imparts Ultrasensitivity in Reaction-Linked Double-Photoswitching Fluorescence Imaging. Journal of the American Chemical Society, 2015, 137, 4312-4315.	13.7	41
68	Efficient green-red piezofluorochromism of bisanthracene-modified dibenzofulvene. RSC Advances, 2015, 5, 1079-1082.	3.6	22
69	Single crystalline nitrogen-doped InP nanowires for low-voltage field-effect transistors and photodetectors on rigid silicon and flexible mica substrates. Nano Energy, 2015, 15, 293-302.	16.0	28
70	Geminal Cross-Coupling of 1,1-Dibromoolefins Facilitating Multiple Topological π-Conjugated Tetraarylethenes. Macromolecules, 2015, 48, 7823-7835.	4.8	33
71	Structural changes in lignin during integrated process of steam explosion followed by alkaline hydrogen peroxide of Eucommia ulmoides Oliver and its effect on enzymatic hydrolysis. Applied Energy, 2015, 158, 233-242.	10.1	44
72	Hyperbranched Self-Immolative Polymers (<i>h</i> SIPs) for Programmed Payload Delivery and Ultrasensitive Detection. Journal of the American Chemical Society, 2015, 137, 11645-11655.	13.7	126

#	Article	IF	CITATIONS
73	Design, synthesis and photoswitching of broad-spectrum fluorescent hexaarylbiimidazoles. RSC Advances, 2014, 4, 64371-64378.	3.6	7
74	Chemical reactivation of quenched fluorescent protein molecules enables resin-embedded fluorescence microimaging. Nature Communications, 2014, 5, 3992.	12.8	99
75	A trident dithienylethene-perylenemonoimide dyad with super fluorescence switching speed and ratio. Nature Communications, 2014, 5, 5709.	12.8	136
76	Stimuliâ€Responsive Nanocomposite: Potential Injectable Embolization Agent. Macromolecular Rapid Communications, 2014, 35, 579-584.	3.9	24
77	Water-Soluble Polymeric Photoswitching Dyads Impart Super-Resolution Lysosome Highlighters. Macromolecules, 2014, 47, 8594-8601.	4.8	40
78	Photocontrolled Intramolecular Charge/Energy Transfer and Fluorescence Switching of Tetraphenyletheneâ€Dithienyletheneâ€Perylenemonoimide Triad with Donor–Bridge–Acceptor Structure. Chemistry - an Asian Journal, 2014, 9, 104-109.	3.3	38
79	Spiropyran-based biodegradable polymer all-optical transistors integrate the switching and modulation of visible light frequency. Chemical Communications, 2014, 50, 2664.	4.1	18
80	A synergy effect between the hydrophilic PEG and rapid solvent evaporation induced formation of tunable porous microspheres from a triblock copolymer. RSC Advances, 2014, 4, 629-633.	3.6	9
81	High performance rigid and flexible visible-light photodetectors based on aligned X(In, Ga)P nanowire arrays. Journal of Materials Chemistry C, 2014, 2, 1270-1277.	5.5	53
82	High-Performance Hybrid Phenyl-C61-Butyric Acid Methyl Ester/Cd ₃ P ₂ Nanowire Ultraviolet–Visible–Near Infrared Photodetectors. ACS Nano, 2014, 8, 787-796.	14.6	82
83	Reversible Fluorescence Switching of Spiropyran-Conjugated Biodegradable Nanoparticles for Super-Resolution Fluorescence Imaging. Macromolecules, 2014, 47, 1543-1552.	4.8	75
84	Tetraphenylethene-decorated carbazoles: synthesis, aggregation-induced emission, photo-oxidation and electroluminescence. Journal of Materials Chemistry C, 2014, 2, 7001-7012.	5.5	53
85	General Synthetic Approach toward Geminal-Substituted Tetraarylethene Fluorophores with Tunable Emission Properties: X-ray Crystallography, Aggregation-Induced Emission and Piezofluorochromism. Chemistry of Materials, 2014, 26, 4433-4446.	6.7	109
86	Direct validation of the restriction of intramolecular rotation hypothesis via the synthesis of novel ortho-methyl substituted tetraphenylethenes and their application in cell imaging. Chemical Communications, 2014, 50, 12058-12060.	4.1	132
87	Condensed state fluorescence switching of hexaarylbiimidazole-tetraphenylethene conjugate for super-resolution fluorescence nanolocalization. Frontiers of Optoelectronics, 2013, 6, 458-467.	3.7	4
88	Optical properties and red to near infrared piezo-responsive fluorescence of a tetraphenylethene–perylenebisimide–tetraphenylethene triad. Journal of Materials Chemistry C, 2013, 1, 6709.	5.5	64
89	Aggregation-induced emission logic gates based on metal ion sensing of phenanthroline–tetraphenylethene conjugates. Journal of Materials Chemistry C, 2013, 1, 7519.	5.5	41
90	Photoswitchable aggregation-induced emission of a dithienylethene–tetraphenylethene conjugate for optical memory and super-resolution imaging. RSC Advances, 2013, 3, 8967.	3.6	97

#	Article	IF	CITATIONS
91	Design, synthesis and optical properties of a green fluorescent photoswitchable hexaarylbiimidazole (HABI) with non-conjugated design. RSC Advances, 2013, 3, 9167.	3.6	19
92	Biodegradable polymer nanoparticles with photoswitchable fluorescence for super-resolution bioimaging. , 2013, , .		0
93	Singleâ€Crystalline pâ€Type Zn ₃ As ₂ Nanowires for Fieldâ€Effect Transistors and Visibleâ€Light Photodetectors on Rigid and Flexible Substrates. Advanced Functional Materials, 2013, 23, 2681-2690.	14.9	79
94	Spiropyran-Based Molecular Photoswitches. Chinese Journal of Organic Chemistry, 2013, 33, 927.	1.3	6
95	Photoswitchable polymer nanoparticles for two-photon excitation fluorescent imaging. , 2013, , .		0
96	Optical Properties and Photoâ€Oxidation of Tetraphenyletheneâ€Based Fluorophores. Chemistry - A European Journal, 2012, 18, 16037-16045.	3.3	91
97	Carbazole oligomers revisited: new additions at the carbazole 1- and 8-positions. RSC Advances, 2012, 2, 10821.	3.6	40
98	Utilising tetraphenylethene as a dual activator for intramolecular charge transfer and aggregation induced emission. Chemical Communications, 2012, 48, 7711.	4.1	147
99	Fluorescence quenching and enhancement of vitrifiable oligofluorenes end-capped with tetraphenylethene. Journal of Materials Chemistry, 2012, 22, 7515.	6.7	128
100	Hierarchical mesostructures of biodegradable triblock copolymers via evaporation-induced self-assembly directed by alkali metal ions. Colloid and Polymer Science, 2012, 290, 1637-1646.	2.1	3
101	Controlled Synthesis and Ti—O Bond Stability of Starâ€Shaped Biodegradable Polyesters via Titanateâ€Initiated ROP of Cyclic Esters at Ambient Temperature. Macromolecular Chemistry and Physics, 2012, 213, 1499-1508.	2.2	8
102	Synthesis and characterization of biodegradable amphiphilic triblock copolymers methoxy-poly(ethylene glycol)-b-poly(L-lysine)-b-poly(L-lactic acid). Journal of Polymer Research, 2012, 19, 1.	2.4	12
103	Microwave synthesis of zinc sulfite and porous zinc oxide microrods. Chemical Communications, 2011, 47, 3986.	4.1	7
104	One-step template-free synthesis of monoporous polymer microspheres with uniform sizes via microwave-mediated dispersion polymerization. Nanoscale, 2011, 3, 4608.	5.6	19
105	PHOTOSWITCHABLE NANOFLUOROPHORES FOR INNOVATIVE BIOIMAGING. Journal of Innovative Optical Health Sciences, 2011, 04, 395-408.	1.0	10
106	Reversible Two-Photon Photoswitching and Two-Photon Imaging of Immunofunctionalized Nanoparticles Targeted to Cancer Cells. Journal of the American Chemical Society, 2011, 133, 365-372.	13.7	168
107	A Convenient Method for the Synthesis of the Amphiphilic Triblock Copolymer Poly(<scp>L</scp> â€lactic acid) <i>â€blockâ€</i> Poly(<scp>L</scp> â€lysine) <i>â€blockâ€</i> Poly(ethylene glyc Monomethyl Ether. Macromolecular Chemistry and Physics, 2011, 212, 563-573.	o\$.2	8
108	Microwave-controlled ultrafast synthesis of uniform silver nanocubes and nanowires. Chemical Physics Letters, 2011, 501, 414-418.	2.6	30

#	Article	IF	CITATIONS
109	Microwave-Controlled Facile Synthesis of Well-Defined PbS Hexapods. Journal of Nanoscience and Nanotechnology, 2011, 11, 7807-7812.	0.9	5
110	Synthesis, selfâ€assembly, drugâ€release behavior, and cytotoxicity of triblock and pentablock copolymers composed of poly(εâ€caprolactone), poly(<scp>L</scp> â€lactide), and poly(ethylene glycol). Journal of Polymer Science Part A, 2010, 48, 4583-4593.	2.3	35
111	Tetrabutyl titanate-controlled polymerization of Îμ-caprolactone at ambient temperature. Chemical Communications, 2010, 46, 5805.	4.1	8
112	Media-Modulated Interchain or Intrachain Coordination of Amphiphilic Block Copolymer Micelles. Macromolecules, 2010, 43, 6156-6165.	4.8	16
113	A stilbene-based fluoroionophore for copper ion sensing in both reduced and oxidized environments. Talanta, 2010, 81, 678-683.	5.5	19
114	The Cytotoxicity of Quantum Dots CdSe/CdS functionalized with -COOH and –NH2. Materials Research Society Symposia Proceedings, 2009, 1220, 6041.	0.1	0
115	Heparinâ^'Paclitaxel Conjugates as Drug Delivery System: Synthesis, Self-Assembly Property, Drug Release, and Antitumor Activity. Bioconjugate Chemistry, 2009, 20, 2214-2221.	3.6	75
116	Microwave-Mediated Nonaqueous Synthesis of Quantum Dots at Moderate Temperature. Langmuir, 2009, 25, 10189-10194.	3.5	28
117	Real-Time Monitoring and Scale-Up Synthesis of Concentrated Gold Nanorods. Journal of Biomedical Nanotechnology, 2009, 5, 573-578.	1.1	5
118	Towards Aqueous Gold Nanoparticles with Buffer Resistance and High Concentration. Journal of Biomedical Nanotechnology, 2009, 5, 536-541.	1.1	1
119	Near-Infrared Quantum Dot Contrast Agents for Fluorescence Tissue Imaging: A Phantom Study. Current Nanoscience, 2009, 5, 160-166.	1.2	4
120	Green Chemistry for Large-Scale Synthesis of Semiconductor Quantum Dots. Langmuir, 2008, 24, 5241-5244.	3.5	53
121	PbS Quantum Dots for Near-Infrared Fluorescence Imaging. , 2008, , .		0
122	CdSe/CdS/SiO ₂ Core/Shell/Shell Nanoparticles. Journal of Nanoscience and Nanotechnology, 2007, 7, 2343-2348.	0.9	22
123	Reversibly Photoswitchable Dual-Color Fluorescent Nanoparticles as New Tools for Live-Cell Imaging. Journal of the American Chemical Society, 2007, 129, 3524-3526.	13.7	338
124	Surface modification and functionalization of semiconductor quantum dots through reactive coating of silanes in toluene. Journal of Materials Chemistry, 2007, 17, 800-805.	6.7	43
125	Spiropyran-Based Photochromic Polymer Nanoparticles with Optically Switchable Luminescence. Journal of the American Chemical Society, 2006, 128, 4303-4309.	13.7	479
126	Zinc ion induced polymorphism in macromolecular self-assembly of diblock copolymers. Talanta, 2005, 67, 525-531.	5.5	2

#	Article	IF	CITATIONS
127	Light-Controlled Molecular Switches Modulate Nanocrystal Fluorescence. Journal of the American Chemical Society, 2005, 127, 8968-8970.	13.7	230
128	Thermosensitive Gold Nanoparticles. Journal of the American Chemical Society, 2004, 126, 2656-2657.	13.7	436
129	A Strategy to Prepare Anemone-Shaped Polymer Brush by Controlled/Living Radical Polymerization. ACS Symposium Series, 2003, , 342-351.	0.5	4
130	An ESR Study of Reversible Additionâ^'Fragmentation Chain Transfer Copolymerization of Styrene and Maleic Anhydride. Macromolecules, 2002, 35, 6739-6741.	4.8	46
131	A unique synthesis of a well-defined block copolymer having alternating segments constituted by maleic anhydride and styrene and the self-assembly aggregating behavior thereof. Chemical Communications, 2001, , 365-366.	4.1	79
132	Fluorescence Enhancement of Dicyanomethylene-4H-Pyran Derivatives in Solid State for Visualization of Latent Fingerprints. Frontiers in Chemistry, 0, 10, .	3.6	3